ARMY RESEARCH LABORATORY

Gun Liner Bond Strength Studies

by William S. de Rosset

ARL-CR-649 **June 2010**

prepared by

Dynamic Science, Inc.
8433 Black Canyon Hwy.
Phoenix, AZ 85021

under contract

W911QX09-C-0057

NOTICES

Disclaimers

The findings in this report are not to be construed as an official Department of the Army position unless so designated by other authorized documents.

Citation of manufacturer's or trade names does not constitute an official endorsement or approval of the use thereof.

Destroy this report when it is no longer needed. Do not return it to the originator.

Army Research Laboratory
Aberdeen Proving Ground, MD 21005-5069

ARL-CR-649 **June 2010**

Gun Liner Bond Strength Studies

William S. de Rosset
Weapons and Materials Research Directorate, ARL

prepared by

Dynamic Science, Inc.
8433 N. Black Canyon Hwy.
Phoenix, AZ 85021

under contract

W911QX09-C-0057

REPORT DOCUMENTATION PAGE	Form Approved OMB No. 0704-0188

1. REPORT DATE *(DD-MM-YYYY)*	2. REPORT TYPE	3. DATES COVERED (From - To)
June 2010	Final	May 2009–March 2010

4. TITLE AND SUBTITLE	5a. CONTRACT NUMBER
Gun Liner Bond Strength Studies	W911QX09-C-0057
	5b. GRANT NUMBER
	5c. PROGRAM ELEMENT NUMBER

6. AUTHOR(S)	5d. PROJECT NUMBER
William S. de Rosset	5e. TASK NUMBER
	5f. WORK UNIT NUMBER

7. PERFORMING ORGANIZATION NAME(S) AND ADDRESS(ES)	8. PERFORMING ORGANIZATION REPORT NUMBER
Dynamic Science, Inc. 8433 N. Black Canyon Hwy. Phoenix, AZ 85021	ARL-CR-649

9. SPONSORING/MONITORING AGENCY NAME(S) AND ADDRESS(ES)	10. SPONSOR/MONITOR'S ACRONYM(S)
U.S. Army Research Laboratory ATTN: RDRL-WMM F Aberdeen Proving Ground, MD 21005-5069	ARL
	11. SPONSOR/MONITOR'S REPORT NUMBER(S)

12. DISTRIBUTION/AVAILABILITY STATEMENT

Approved for public release; distribution is unlimited.

13. SUPPLEMENTARY NOTES

14. ABSTRACT

Experiments have been conducted in order to see if internal grooves in steel cylinders will lead to higher bond strengths produced by the GLEEM (Gun Liner Emplacement with an Elastomeric Material) process. Groove depth and twist angle were varied. Both experimental and analytical studies showed that at the pressures used, there was little movement of the liner material into the grooves. However, the liner was seen to conform to very small machining marks in the steel cylinder inner bore, providing an increase in the coefficient of friction. A second significant finding was that using Teflon (Teflon is a registered trademark of DuPont Corp, Wilmington, DE) as the elastomer reduced the friction between the elastomer and liner, giving a more even pressure distribution along the length of the cylinder.

15. SUBJECT TERMS

gun tube liner, bond strength, elastomer, plastic deformation, Stellite 25

16. SECURITY CLASSIFICATION OF:			17. LIMITATION OF ABSTRACT	18. NUMBER OF PAGES	19a. NAME OF RESPONSIBLE PERSON
a. REPORT	b. ABSTRACT	c. THIS PAGE			William S. de Rosset
Unclassified	Unclassified	Unclassified	UU	38	19b. TELEPHONE NUMBER (*Include area code*) (410) 306-0816

Standard Form 298 (Rev. 8/98)
Prescribed by ANSI Std. Z39.18

Contents

List of Figures

List of Tables

Acknowledgments

The author wishes to thank David Gray, who ran the Instron machine, collected the data, and carried out the bond strength measurements. The author also thanks Mica Gallagher for using the EDM machine to cut the cylinders and for making all the hardness measurements. Finally, the author acknowledges the technical advice received from James Bender, U.S. Army Research Laboratory (ARL) and Scott Marinus (Mallett Technology) in carrying out the ANSYS calculations.

1. Introduction

A process has recently been developed to emplace metallic liners in gun tubes called GLEEM (Gun Liner Emplacement with Elastomeric Materials) (*1*, *2*). The purpose of the liner is to increase the useful life of the gun tube. The process consists of filling the liner with an elastomeric material, inserting the liner into the gun barrel, and applying a load to the elastomer that is high enough to plastically deform both the liner and the gun tube. The residual radial stress generated by this operation induces a frictional bond between the liner and gun tube. The process currently is patent pending (*3*).

The bond strength produced by this process is the primary measure of its success. Frictional bonds with strengths of 13.8 MPa (2000 psi) have been achieved on some of the first lined tubes examined (*2*). This bond strength is much lower than that achieved through explosive bonding, which produces bond strengths on the order of the liner's material yield strength (*4*). Explosive bonding requires a material have good ductility. Other materials may make better liners but do not possess sufficient ductility for the explosive bonding process. The GLEEM process does not require much ductility in the liner material and is therefore a possible option for emplacing liner materials of all types in gun tubes. However, more work needs to be done to increase the strength of the bond that is achieved with this technique.

Since the bond that is produced by the GLEEM process is frictional, any changes in the surface roughness of either the liner or gun tube will affect the bond strength. A series of experiments was undertaken to increase the bond strength by machining grooves in the steel cylinder. The experimental procedures used to do this are presented in the next section. The results of those experiments are presented in section 3. Extensive modeling of the deformation of both the steel and Stellite 25 liner were undertaken using the ANSYS* finite element code. The calculated results are compared to selected experimental results in section 4. Section 5 contains the discussion, and the final section provides a summary of the work.

2. Experimental Procedures

Experiments were undertaken to see if an increased bond strength could be achieved in the GLEEM process by grooving the inside surface of the steel tube. The grooves would provide a mechanical lock between the liner and gun tube as the liner plastically deformed.

The GLEEM process is explained in detail in reports by de Rosset (*2*) and Gray (*5*). A schematic of the test setup is shown in figure 1.

*ANSYS is a registered trademark of ANSYS Corp., Canonsburg, PA.

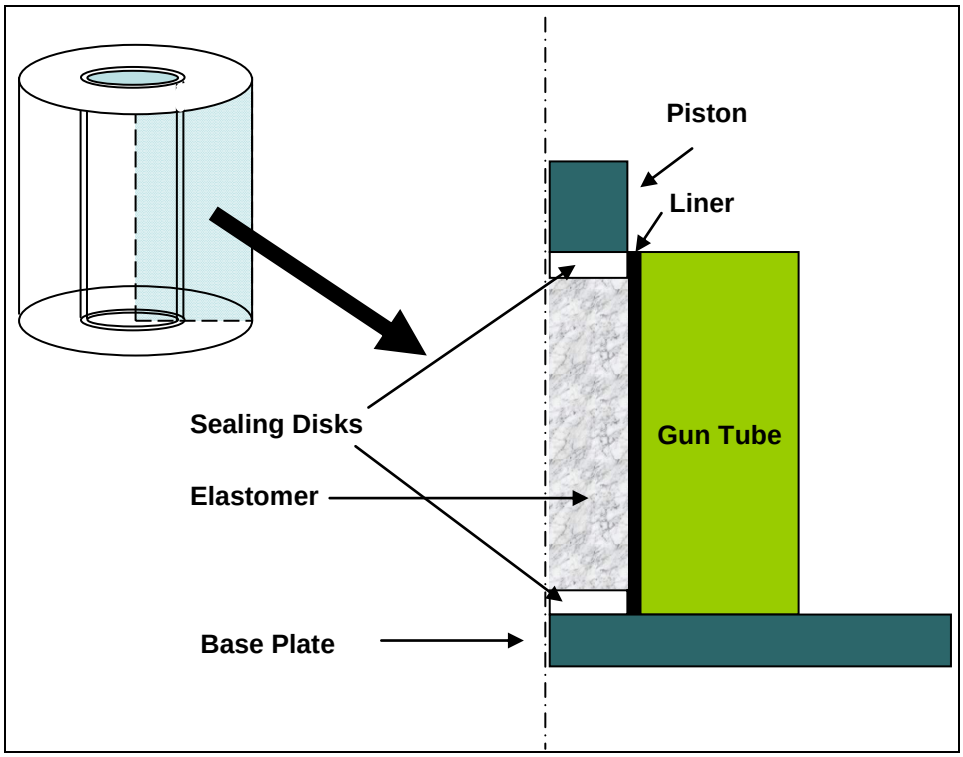

Figure 1. Schematic of GLEEM test setup.

The liner is filled with an elastomeric or other easily deformable material, and then the filled liner is placed in the gun tube. The elastomeric material is sealed at the top and bottom with nylon disks. This arrangement is placed in a load frame, and pressure is applied to the elastomeric material with a piston. The pressure causes the elastomeric material to expand radially. If the pressure is high enough, the liner and steel cylinder deform plastically, leaving a residual stress that produces a frictional bond between the liner and gun tube.

During the course of this work, procedures for conducting the experiments and gathering the data changed significantly. There was an initial study to determine the effect of groove depth on the bond strength. Based on these tests, a second set of experiments was conducted using two materials for the elastomer. In addition, measurements of hoop strain went from a single strain gage to Digital Image Correlation (DIC) that provided strain data over a large portion of the external steel cylinder surface. (See Chu, et al. [6] for a discussion of DIC theory and practice.)

2.1 Initial Experiments

For the initial study, four 127-mm (5-in) long 4340 steel cylinders were heat treated with the goal of achieving a yield strength of 1.1×10^3 MPa (160 ksi). This is the yield strength specified for the M242 gun barrel. The inside surfaces of the steel cylinders were machined according to the spiral pattern shown in figure 2. The dashed slanted lines indicate the internal grooves. The spiral pitch is 51 mm (2 in).

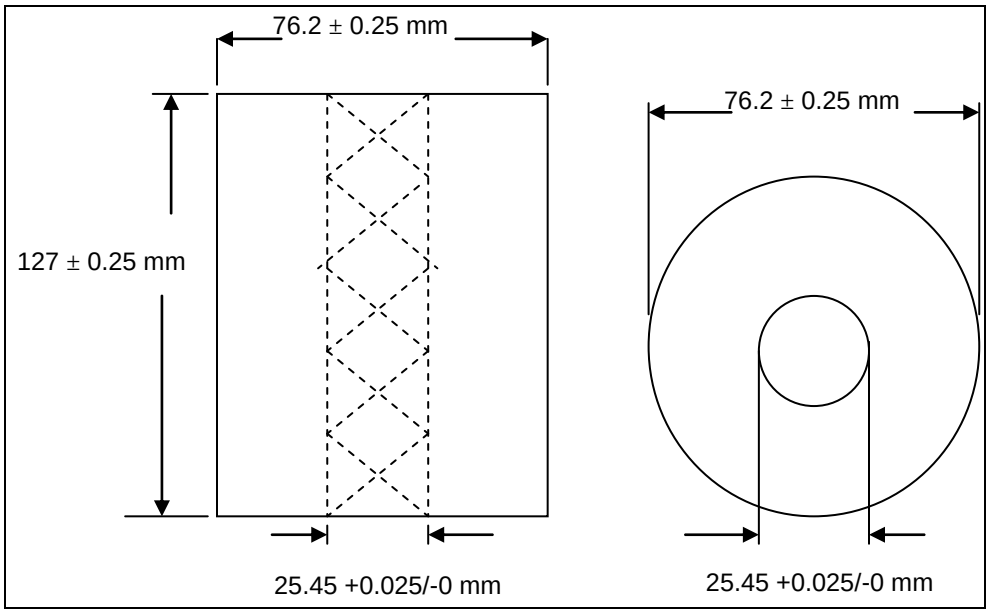

Figure 2. Steel cylinder with scored internal surface.

Each cylinder was made with a different groove depth. For this study, groove depths of 0.127, 0.254, 0.381, and 0.508 mm (5, 10, 15, and 20 mil) were used. The grooves were made with a standard metal-cutting tool.

Stellite 25 tubes were made to fit the steel cylinders. The tubes were 127-mm long and had an outer diameter of 25.4±0.05 mm and an inner diameter of 20.57 ± 0.05 mm. Elastomer plugs and nylon seals were made for all four tubes. The upper seal was made 19-mm (3/4-in) long in the expectation that high loads would be used for these tests. A single hoop strain gage was attached at the mid-point on the outer surface of each steel cylinder.

The yield strength of the Stellite 25 is ~8.95×10^2 MPa (130 ksi). Using a hydrostatic approximation, a load F applied to the elastomer produces a pressure P on the Stellite liner given by

$$P = F/(\pi r^2), \tag{1}$$

where r is the inner radius of the liner. A load of 2.94×10^5 N (66,000 lb) must be applied for r = 10.3 mm in order to exceed the yield strength of the Stellite 25 liner.

The cylinder with 0.127-mm grooves was processed first. A 76-mm long normalized steel pusher was used for the tests with this cylinder. The cross-head speed of the load frame was set to 0.1 in/min. After about 15 min, the pusher appeared to be cocked and bent. The test was stopped and the pusher removed from the Stellite 25 liner. A maximum load of 5.36×10^5 N (120480 lb) was achieved. However, this load was probably put on the Stellite liner and not the elastomer plug. Consequently, the maximum load on the liner is unknown.

A new pusher replaced the bent pusher. The length of the new pusher was 44.5 mm (1.75 in), and it was heat treated to HRC 43. The cylinder with the 0.254-mm deep grooves was processed. The load frame software was to ramp the load up to 4.67×10^5 N at cross-head speed of 0.1 in/min. However, a malfunction occurred, and the load overshot to 4.95×10^5 N (111326 lb). It was brought down and manually cycled between 4.54×10^5 N (102,000 lb) and 4.80×10^5 N (108,000 lb) for the next hour. During this time, the displacement of the steel pusher was manually adjusted in an attempt to keep the load constant. The final displacement of the pusher was 25 mm.

The next cylinder tested had groove depths of 0.381 mm (15 mil). This time the load control was used, and the load was smoothly ramped to 4.67×10^5 N (105,000 lb) at 2.22×10^4 N/min. The load was maintained at 4.67×10^5 N for an hour by setting the appropriate software controls that governed the operation of the load frame. The cylinder with the 0.508-mm deep grooves was processed next. This time, the load rate was 3.11×10^4 N/min. The load was maintained at 4.67×10^5 N for an hour. Finally, the cylinder with the 0.127-mm deep grooves was processed. For this test, an upper seal that was only 12.7-mm long was used. The load was taken to 4.67×10^5 N and maintained for an hour.

After the Stellite 25 liners had been pressed into the steel cylinders, the inner diameter of each Stellite 25 liner was measured as a function of position along the cylinder axis. The steel cylinders were then sectioned with an electro-spark discharge machine in order to measure the bond strength. Figure 3 shows where the sectioning took place. Each ring sample was 5.08-mm thick. The bond strengths were measured for each cylinder according to the procedure presented in Carter, et al. (*3*).

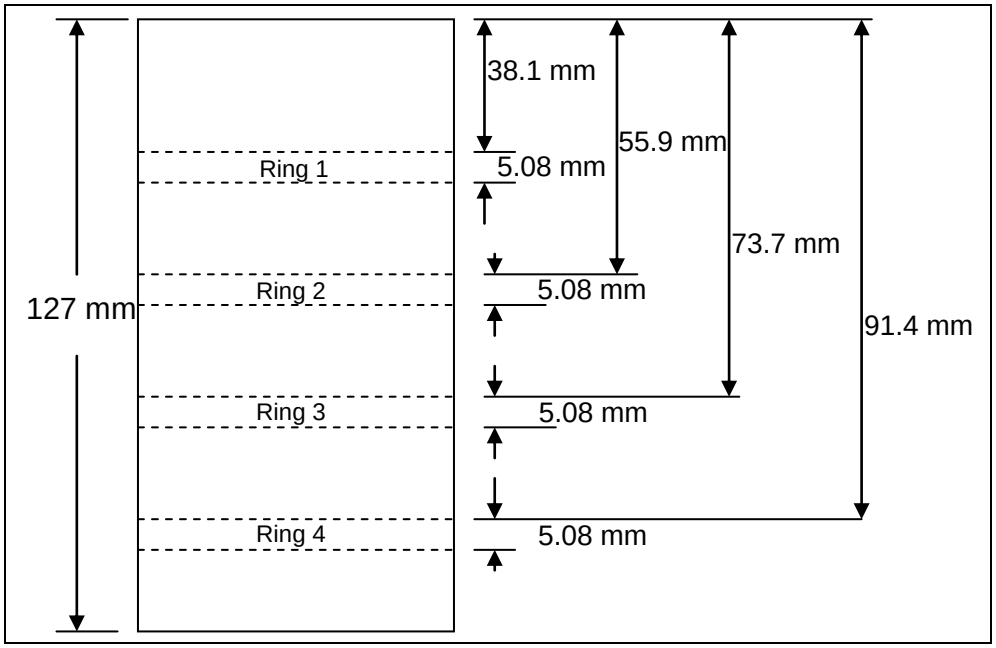

Figure 3. Sectioning locations for first four cylinders.

Other information was gathered on the four cylinders after the bond strength measurements had been made. The cylinder's hardness was measured using the third ring of each cylinder. The outer diameters of the sectioned cylinders were also measured as a function of axial position. Finally, the portions of the Stellite 25 tube contained in the top-most portion of each steel cylinder were removed by an EDM machine. The cut was made from the inner surface outwards so that the steel cylinder was left intact. Photographs were taken of the Stellite 25 liner sections.

2.2 Follow-up Experiments

Test procedures were adjusted to take into account information obtained from the initial series of tests. For the follow-up series of tests, three 4340 steel cylinders with dimensions the same as those shown in figure 1 were made. Each cylinder had a double-spiral pattern of grooves machined into the inner diameter to a depth of 0.254 mm (10 mil). The spiral pattern was tighter than the previous one, with one complete revolution occurring every 21-mm of travel down the cylinder. The steel cylinders were heat treated with the goal of achieving a yield strength of 1.1×10^3 MPa. Hardness measurements were made on the top surface of each steel cylinder before the GLEEM processing took place.

The first steel cylinder was processed in the same way as the previous four cylinders. The elastomeric material was Dow Corning Silastic* JRTV, and erucic acid was used as a high-pressure lubricant between the elastomer and Stellite 25 tube. It was not known before the tests what load would cause failure of the nylon seals. Therefore, the load was initially set at 3.56×10^5 N (80,000 lb) and then released. At this load, the seals held. Next, the load was brought to 4.00×10^5 N (90,000 lb). Here the seals also held. This procedure was continued until a load of 5.34×10^5 N (120,000 lb) was reached. Each load level was applied for 15 min. At the end of the process, a portion of the upper nylon seal was observed to have extruded past the steel piston. However, there was a sufficient amount of the nylon seal remaining to maintain the pressure on the elastomer.

After the GLEEM process had been carried out, measurements of the inner diameter of the Stellite 25 tube were made. The steel cylinder was sectioned according to the cut locations shown in figure 3. Push-out tests were conducted on the rings to measure the bond strength. In addition, the Stellite 25 liner at the bottom of the sample was removed from the steel cylinder and photographed.

The final two procedures employed Teflon† as the elastomeric material. An initial attempt was made to pressurize the cylinder without any nylon seals. However, at a load of 3.24×10^5 N the Teflon extruded past the steel pusher to such an extent that the test had to be stopped. The test was restarted with nylon seals. The length of the top seal for these tests was 12.7 mm. The initial load was ramped to 5.34×10^5 N (120,000 lb). The load was then raised to 6.23×10^5 N

*Silastic is a registered trademark of Dow Corning, Midland, MI.

†Teflon is a registered trademark of DuPont Corp, Wilmington, DE.

(140,000 lb) through a series of 8.9×10^4 N (20,000 lb) increments. The load was held for 15 min at each load level. The final cylinder was processed in a manner similar to that used for the previous one, except that the load was ramped directly to 6.23×10^5 N.

After the tests, the inner diameter of the Stellite 25 tube was measured. The steel cylinder was then sectioned according to the cut locations shown in figure 4. Bond strength measurements were made on the cut samples.

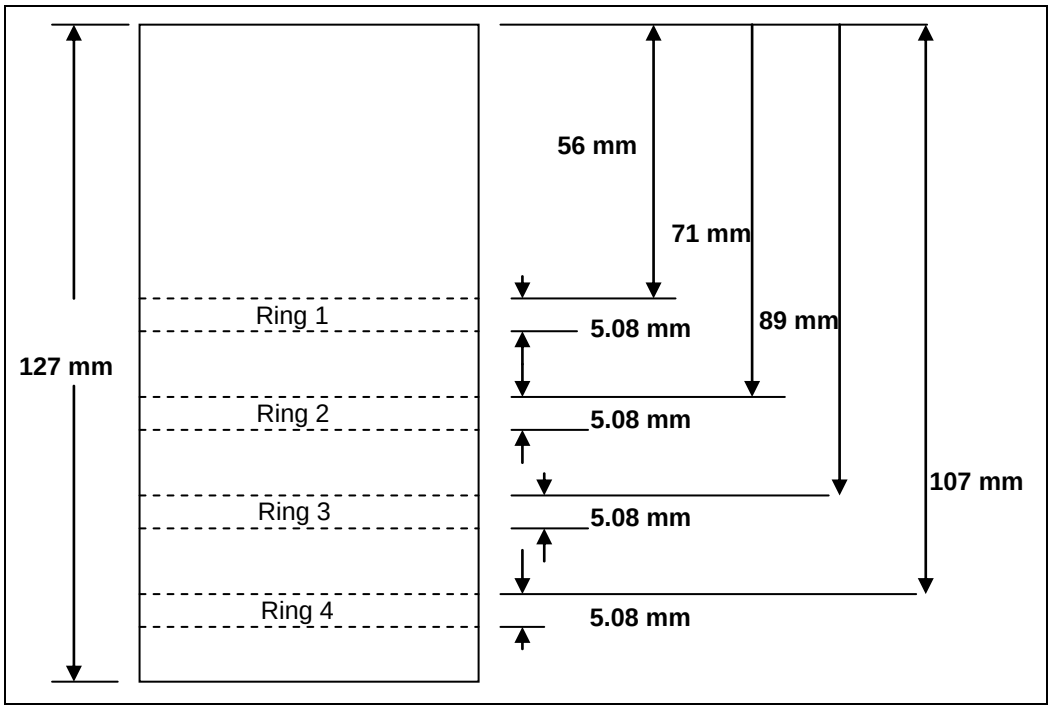

Figure 4. Cylinder sectioning locations for final two cylinders.

As previously mentioned, the hoop strain on each of the last three cylinders was measured with DIC. This technique involves coating a section of the cylinder with a black-and-white speckle pattern. This pattern is then viewed by two cameras as the load is applied to the elastomer in the cylinder. The two images are processed with software that calculates the relative displacement field and therefore the strain field. For our purposes, the hoop strain was only used for investigation. Other components of strain can also be determined from the image correlations. The advantage of the DIC system is that it allows a strain measurement to be taken over a large area of the sample, in contrast to a strain gage that measures the strain in one place.

Bond strengths were measured with the standard push-out tests for each of the rings of the cylinders as detailed in the report by de Rosset et al. (*4*). A malfunction occurred with the EDM in sectioning the last two cylinders. The third ring from the top for both cylinders was cut on an angle that made it impossible to get a correct reading. Consequently, only three rings were used for the bond strength calculation for the last two cylinders.

Table 1 summarizes the test matrix. The cylinders have been numbered for easy reference.

Table 1. Test matrix.

Cylinder No.	Groove Depth (mm)	Groove Twist Rate (mm)	Maximum Load (10^5N)	Elastomer	Strain Measurement
1	0.127	1 in 51	4.67	Silastic	Strain gage
2	0.254	1 in 51	4.95	Silastic	Strain gage
3	0.381	1 in 51	4.67	Silastic	Strain gage
4	0.508	1 in 51	4.67	Silastic	Strain gage
5	0.254	1 in 21	5.34	Silastic	DIC
6	0.254	1 in 21	6.23	Teflon	DIC
7	0.254	1 in 21	6.23	Teflon	DIC

3. Results

Five hardness measurements were taken on each cylinder on the Rockwell C scale. These measurements are shown in table 2 along with an average hardness and a conversion to yield strength by interpolating tabular data from the www. carbidedepot.com Web site (*7*). The measurements indicate that there was a difference in the material strength between the first and second set of cylinders tested. However, each of the cylinders had a hardness value higher than the target hardness of 1100 MPa.

Table 2. Hardness measurements (HRC).

Cylinder No.	Ring 1	Ring 2	Ring 3	Ring 4	Ring 5	Average Hardness (HRC)	Yield Strength (MPa)
1	40.3	41.9	43.1	42.2	42.8	42.1	1319
2	41.6	43.8	41.2	43.1	42.2	42.4	1329
3	43.6	42.7	44.2	44.4	43.4	43.7	1369
4	41.9	41.7	40.7	40.2	43.9	41.7	1307
5	39.0	37.5	38.4	34.0	37.4	37.3	1170
6	37.6	37.6	35.8	35.6	35.1	36.3	1141
7	37.6	37.2	37.3	36.8	39.1	37.6	1180

The hardness difference between the first four and last three cylinders, as well as the applied loads, resulted in different deformations of the inner diameter of the Stellite 25 liners. The inner diameters for the first four liners are presented in figure 5. (The starting point is taken at the top of the cylinder for this and subsequent figures.) Note that in this figure there appears to be a maximum in the inner diameter at the final position of the end of the piston, located ~25 mm from the top of the cylinder.

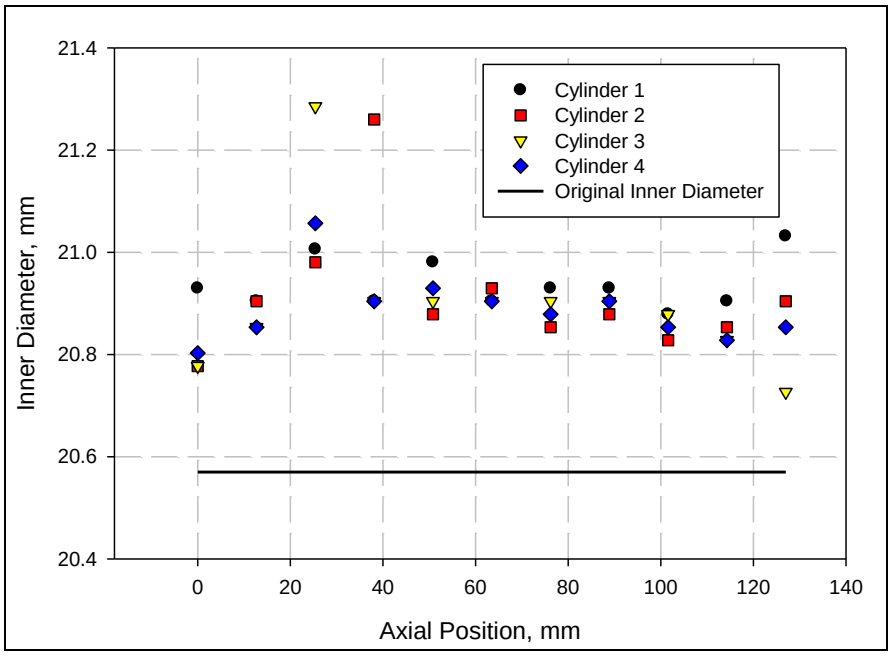

Figure 5. Inner diameter measurements of the first four cylinders as a function of axial position.

Upon examination of the portion of the Stellite 25 liner that was removed from the top section of each cylinder, it was observed that the Stellite 25 liner was embossed in the pattern of the grooves in the steel. This was most pronounced at 25 mm from the top of the tube where the most radial expansion occurred. A picture of the top section of the Stellite 25 liner removed from cylinder 4 is shown in figure 6. Note also faint traces of the machine marks that were made in the steel cylinder and then transferred to the Stellite 25.

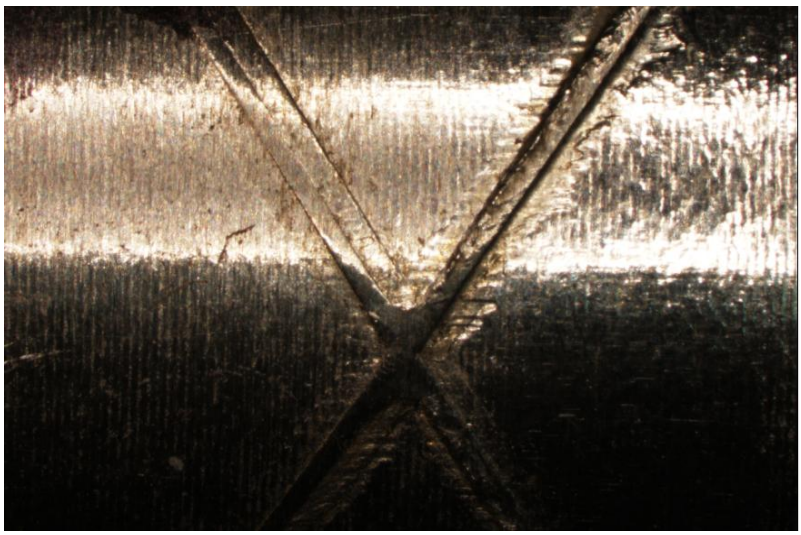

Figure 6. Embossed Stellite liner taken from cylinder 4.

The inner diameter measurements for the last three cylinders are shown in figure 7. Included in this figure is a line that represents the original inner diameter of the Stellite 25 liner, as specified in the procurement document. Measurements made at the ends of the original liner confirmed the specified value. There was an eccentricity noticed with cylinder 7, so two sets of measurements were made, 90° from each other. The diameters were nominally larger than 21 mm, in contrast to the first four cylinders. In addition, there was no pronounced maximum of the inner diameter at the location of the piston's maximum displacement, 25 mm from the top of the cylinder.

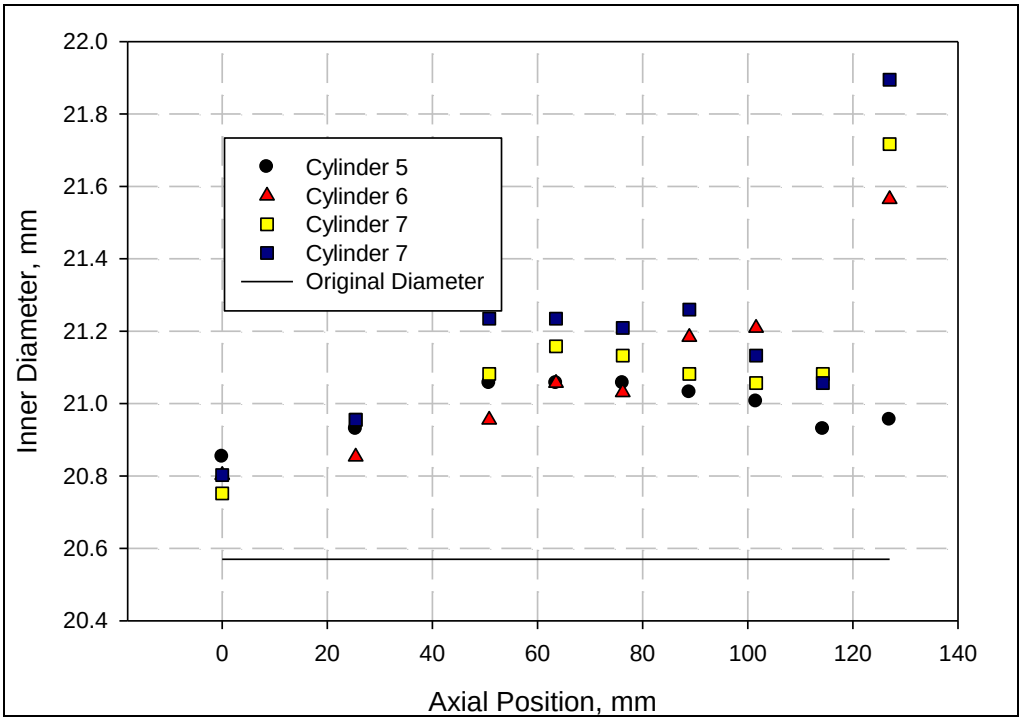

Figure 7. Inner diameter measurements for the last three cylinders as a function of axial position; two separate measurements were made on cylinder 7 at 90° to each other.

The bottom portions of the Stellite 25 tubes were removed from the steel cylinders and examined. The Stellite 25 tube taken from cylinder 6 is shown in figure 8. The markings produced by the grooves in the steel cylinder are barely visible. The machine markings that were made in drilling hole in the steel cylinder can also be seen.

As a final check on the amount of plastic deformation that each of the cylinders underwent, the final outer diameter of the steel cylinder was measured as a function of axial position. These measurements are presented in figure 9. Simple spline curves have been put through the actual data points to facilitate visualization. The maximum outer diameter for each cylinder correlates roughly to the maximum load applied to the elastomer in each case.

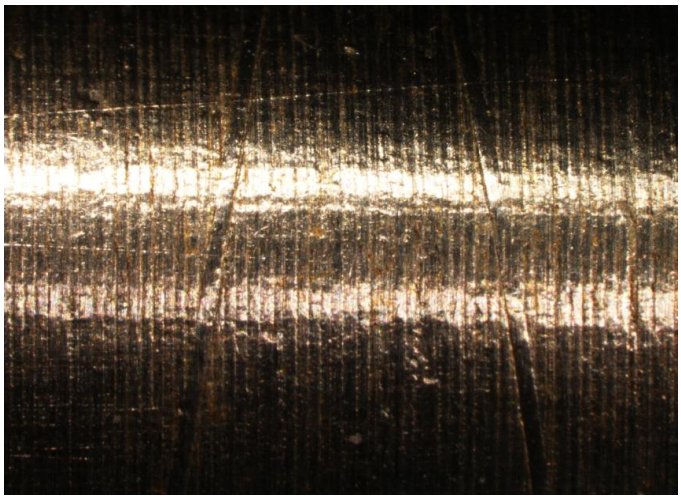

Figure 8. Embossed Stellite liner taken from cylinder 6.

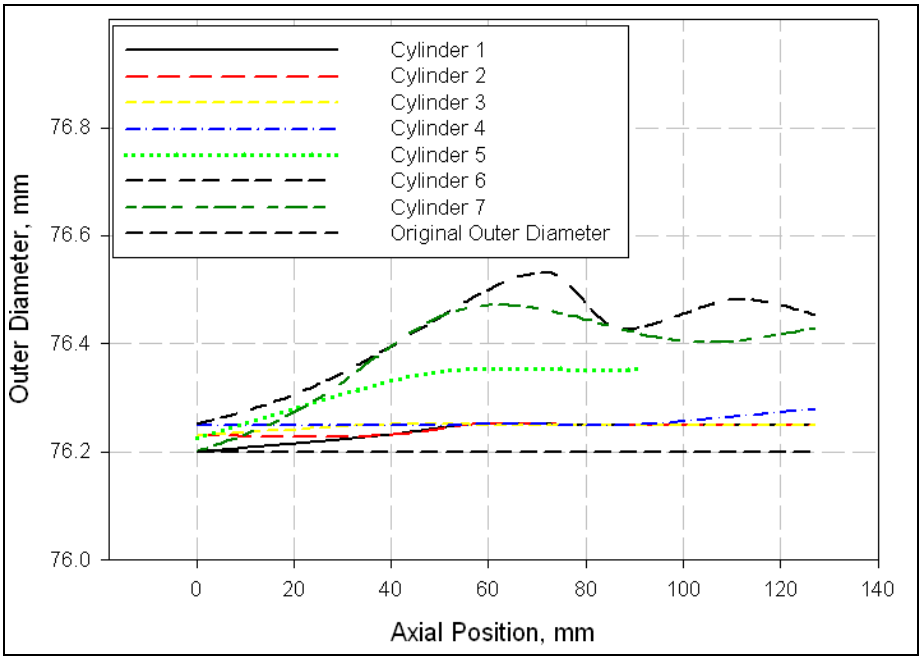

Figure 9. Outer diameter measurements.

The hoop strain measurements made from the strain gage at a single point for cylinders 1–4 was recorded as a function of time. From these data, the maximum hoop strain was identified for each cylinder. These data are shown in table 3. Also shown are the loads that were applied at the time the maximum hoop strain was achieved. This is not always equal to the maximum load, since the piston had to be adjusted to maintain a constant load. The data for cylinder 1 were taken from the second run.

Table 3. Maximum hoop strains for cylinders 1–4.

Cylinder No.	Maximum Hoop Strain (%)	Load at Maximum Strain (10^5N)
1	0.1236	4.67
2	0.1199	4.69
3	0.1131	4.69
4	0.1256	4.69

The hoop strain data recorded at each of the four load levels applied to cylinder 5 are shown in figure 10. The raw data show a negative strain for the first load level near the top of the cylinder. The DIC measurement technique is not highly accurate for very small strains. In actuality, the strain should have been positive.

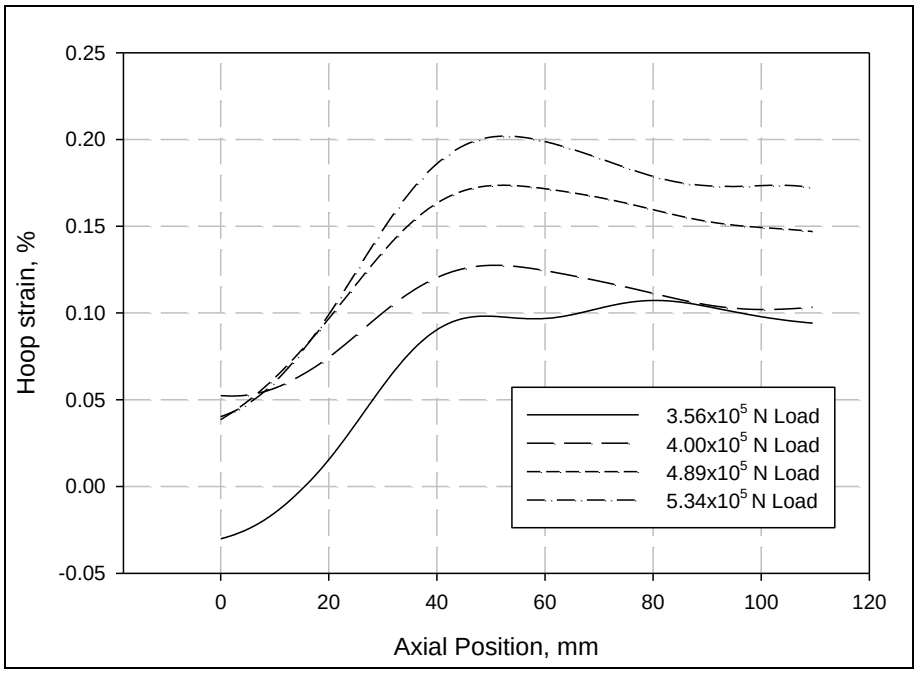

Figure 10. Hoop strain as a function of axial position for various loads applied to cylinder 5.

Similar plots for cylinder 6 are shown in figure 11.

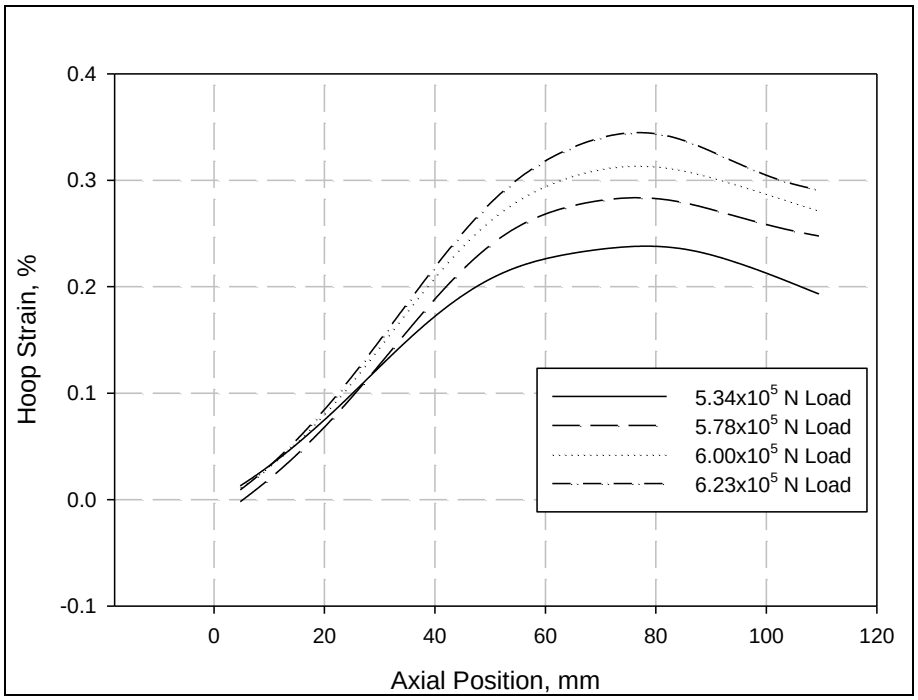

Figure 11. Hoop strain as a function of axial position for various loads applied to cylinder 6.

Data were taken only for the 6.23×10^5 N load for cylinder 7. These data are shown in figure 12.

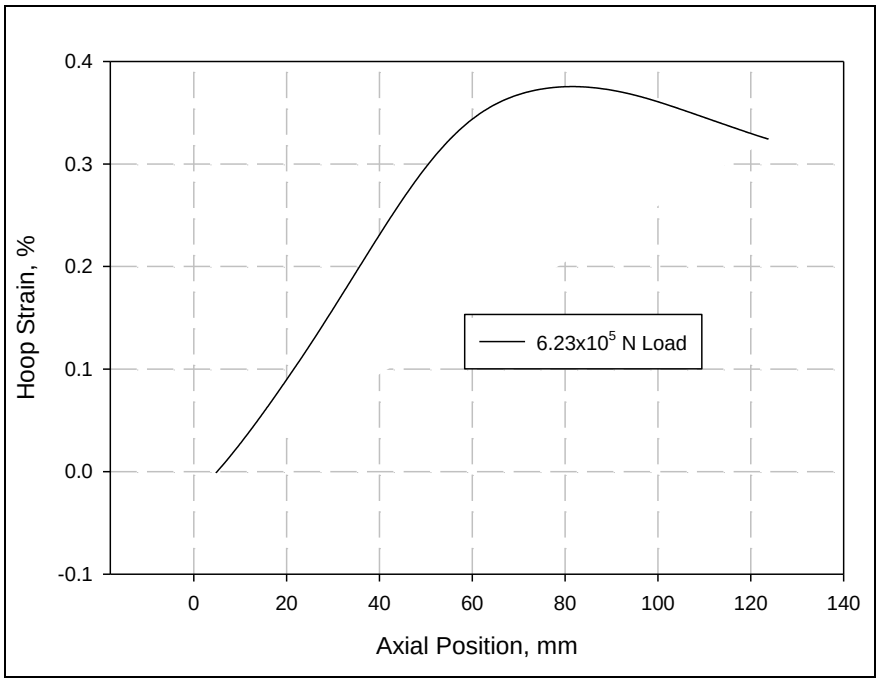

Figure 12. Hoop strain as a function of axial position for cylinder 7.

Bond strength measurements are given in detail in the appendix. The pieces of equipment used to make these measurements (micrometer, load machine) were calibrated in inches and pounds. These measurements are shown and then converted to Standard International (SI) units in the appendix. Table 4 provides a summary of the measurements along with averages and standard deviations. The rings of the cylinder are numbered starting from the top of the cylinder.

Table 4. Bond strength measurement summary.

Cylinder No.	Ring No.	Bond Shear Strength (MPa)	Average Bond Strength (MPa)	Standard Deviation (MPa)
1	1	28.96	23.5	4.5
	2	17.21		
	3	21.47		
	4	26.34		
2	1	33.74	31.6	8.5
	2	43.61		
	3	29.16		
	4	19.89		
3	1	18.05	16.8	0.9
	2	16.59		
	3	15.58		
	4	16.96		
4	1	16.13	18.2	2.4
	2	22.23		
	3	16.60		
	4	17.69		
5	1	26.87	31.2	2.9
	2	32.83		
	3	30.29		
	4	34.89		
6	1	32.17	32.4	0.7
	2	31.60		
	4	33.39		
7	1	22.86	26.5	4.6
	2	27.53		
	4	29.19		

4. Modeling

The ANSYS finite element code was used to model the deformation of the steel cylinder. Two separate models were used. The first examined the deformation of the whole cylinder, and the second was used to estimate the amount of local deformation of the Stellite 25 liner into the groove for a given pressure. Lastly, plasticity theory was used to estimate the internal pressure necessary to yield the entire cylinder.

4.1 Steel Cylinder

Modeling of the GLEEM process was undertaken with ANSYS in an attempt to estimate the extent of frictional effects between the elastomeric material and the Stellite 25 tube. This was done by modeling the cylinder as a friction-free system and comparing the results to the experimental data. While the attempt was made to reduce the friction between the elastomer and Stellite liner in the experiments, it could not be eliminated. Any friction that remained would result in a pressure decrease from the end of the piston to the bottom of the cylinder. A large frictional effect would then produce a significant reduction in the measured hoop strain at the bottom of the cylinder. Since the model did not include frictional effects, a large difference between the calculated and observed hoop strains would be an indication of a large frictional effect.

The model represented a 4340 steel cylinder with a central bore hole. The length of the cylinder was 127 mm (5 in), and its outer diameter was 76.2 mm (3 in). The diameter of the bore hole was 20.57 mm (0.810 in). A picture of the model is shown in figure 13. Since Stellite 25 and 4340 steel have approximately the same Young's modulus, and since the liner was so thin (2.54-mm thick), the liner was not included in the finite element model.

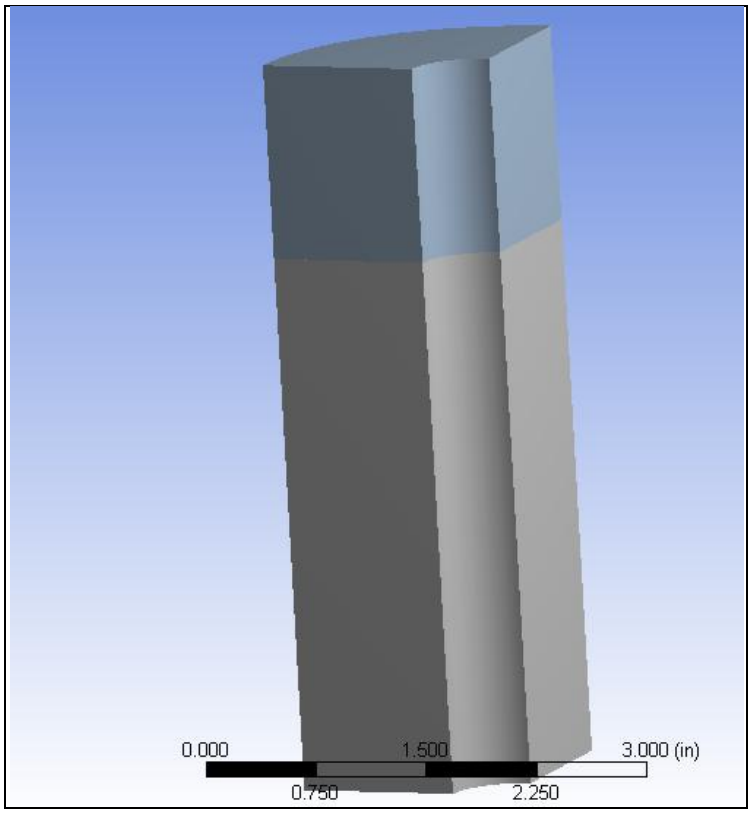

Figure 13. Geometric model of steel cylinder.

The model of the cylinder is partitioned into two sections, shown by the different coloring in the figure. The separation into two sections allows for easy distinction between the upper section of the cylinder that is not pressurized and the lower section that is pressurized. The length of the upper section of the cylinder depends on the applied load, as found experimentally. The larger the load is, the more the piston is displaced. For the first four cylinders, 25 mm was used as the length of the top section. For the remaining three cylinders, a length of 31 mm was used.

Symmetry conditions were imposed by frictionless supports on the symmetry planes (x–z planes) of the model.

In the actual experiment, the ends of the cylinder were restrained from moving by the test fixture. However, the restraints were not perfect. Several simple end conditions for the model were examined. None of them fit the experimental conditions perfectly, but having the ends free to move in the model appeared to give the most reasonable results.

A bilinear isotropic hardening model was used for the 4340 steel. For the first four cylinders, the yield stress was set at 1.33×10^{9} Pa, while a value of 1.16×10^{9} Pa was used for the last three cylinders. These values are based on the hardness measurements taken on the steel cylinders. The default modulus was 2.0×10^{11} Pa (29000 ksi). Several values of the slope of the stress-strain curve past the 0.2% yield point were tried, with no significant difference seen in the results.

A uniform pressure was applied to the bore hole surface on the lower section of the model. The value of P was estimated from equation 1. F was the measured load and r was the radius of the bore hole. For the first four cylinders, a load of 4.69×10^{5} N was used. Two separate calculations were done for the last three cylinders using loads of 5.34×10^{5} N and 6.23×10^{5} N. All loads resulted in pressures that were in excess of the yield point of the steel.

The hoop strain was recorded as a function of the axial position along the outer surface of the steel cylinder. The results of the ANSYS calculation for the first four cylinders are shown in figure 14, along with four data points taken from the strain gages located at the centers of the cylinders.

Figure 15 contains similar comparisons between the calculated results and data for cylinders 5 and 6. The load applied in this case was 5.34×10^{5} N, resulting in an applied pressure of 1405 MPa. Finally, figure 16 contains a comparison of the calculated and experimental results for cylinders 6 and 7 for a load of 6.23×10^{5} N.

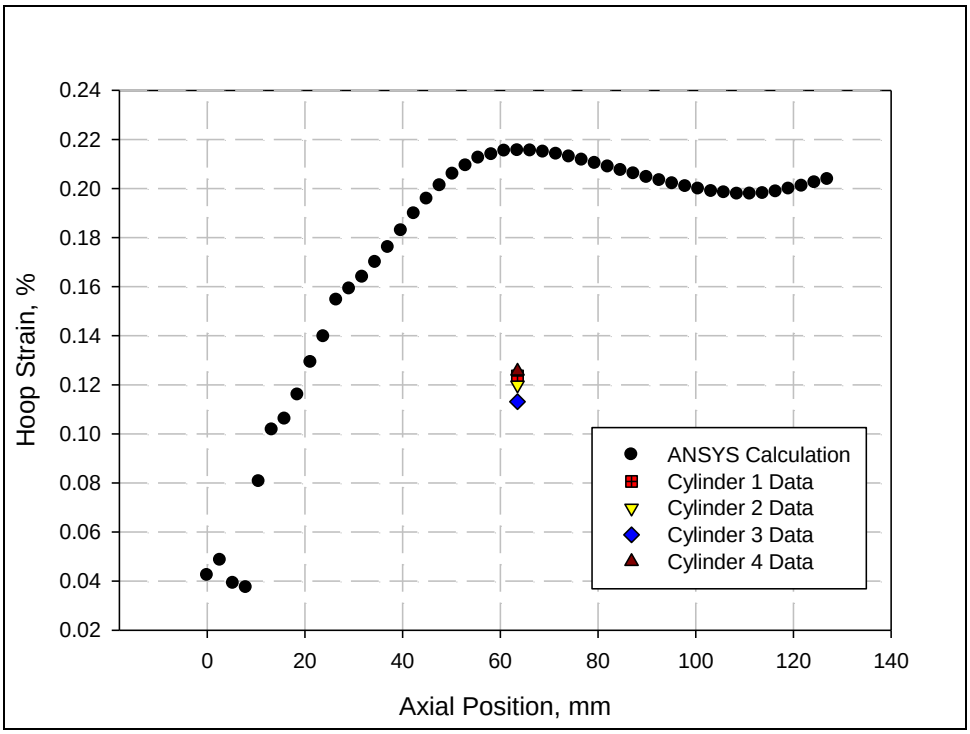

Figure 14. Calculated hoop strain versus axial position for cylinders 1–4; colored points represent data taken from strain gages.

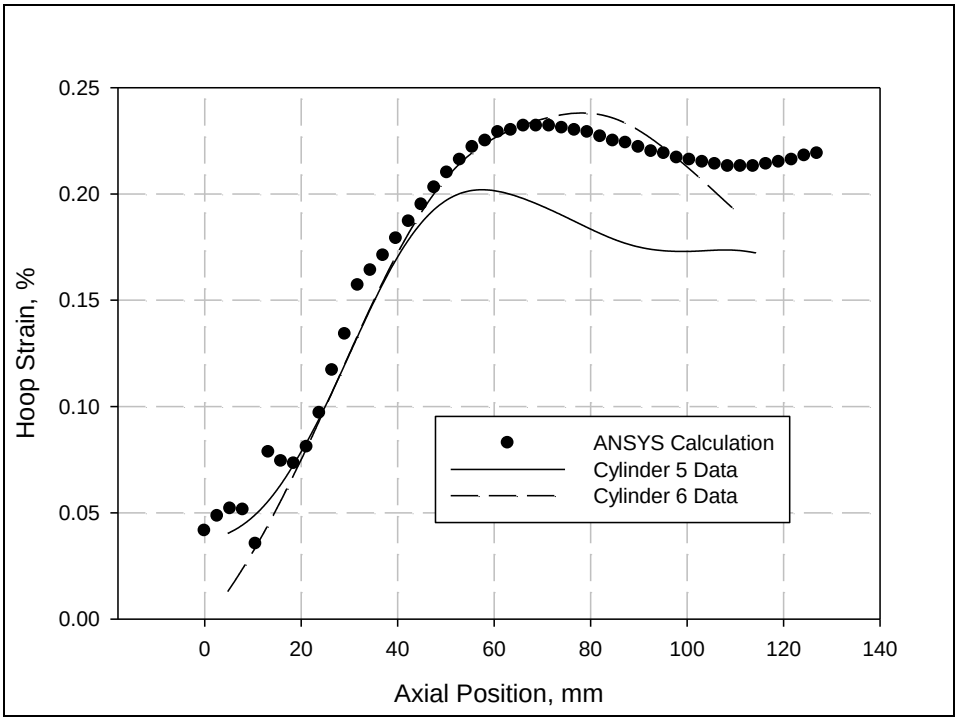

Figure 15. Comparison of calculated and experimental results for a load of 5.34×10^5 N.

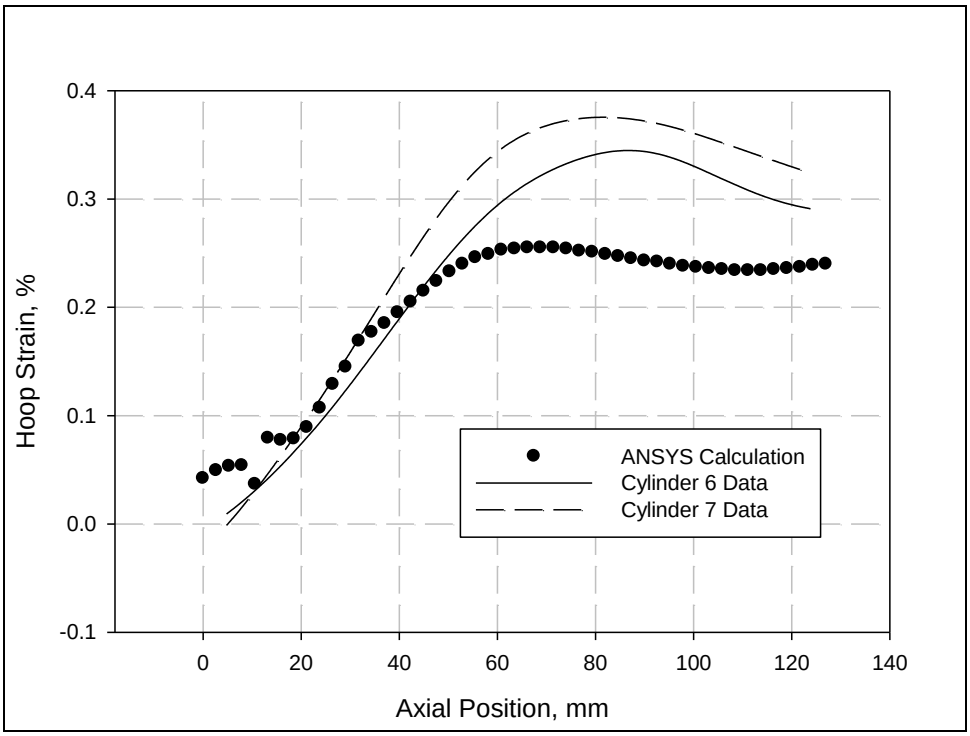

Figure 16. Comparison of calculated and experimental results for a load of 6.23×10^5 N.

4.2 Stellite 25 Deformation into the Groove

The ANSYS finite element code was used to estimate the amount of Stellite 25 deformation into the groove in the steel cylinder as a function of applied pressure. Since the yield strength of Stellite 25 is 8.96×10^2 MPa (130 ksi), it was expected that this would be the threshold radial stress (pressure) necessary to begin the deformation process.

The model used for this analysis is shown in figure 17. Rather than have the cylindrical geometry of the actual liner configuration, the model was simplified to a flat plate. It consists of a Stellite 25 block lying on top of two structural steel blocks. The gap width between the two steel blocks is 0.254 mm (0.010 in). This gap represents the groove. Note the orientation of the global coordinate system shown in this figure. A bilinear stress-strain curve modeled the plastic behavior of the Stellite 25. The yield strength was taken as 8.96×10^2 MPa, and the tangent modulus was set at 5×10^2 MPa.

A uniform pressure is applied to the top face of the Stellite 25 block. In reality, the radial stress in the Stellite 25 liner drops off as a function of distance from the point of load application. Since the Stellite 25 block used in the model is 2.54-mm (0.10-in) thick, the difference between the normal stress at the interface between the Stellite 25 and the steel cylinder is small in comparison to the actual experiment.

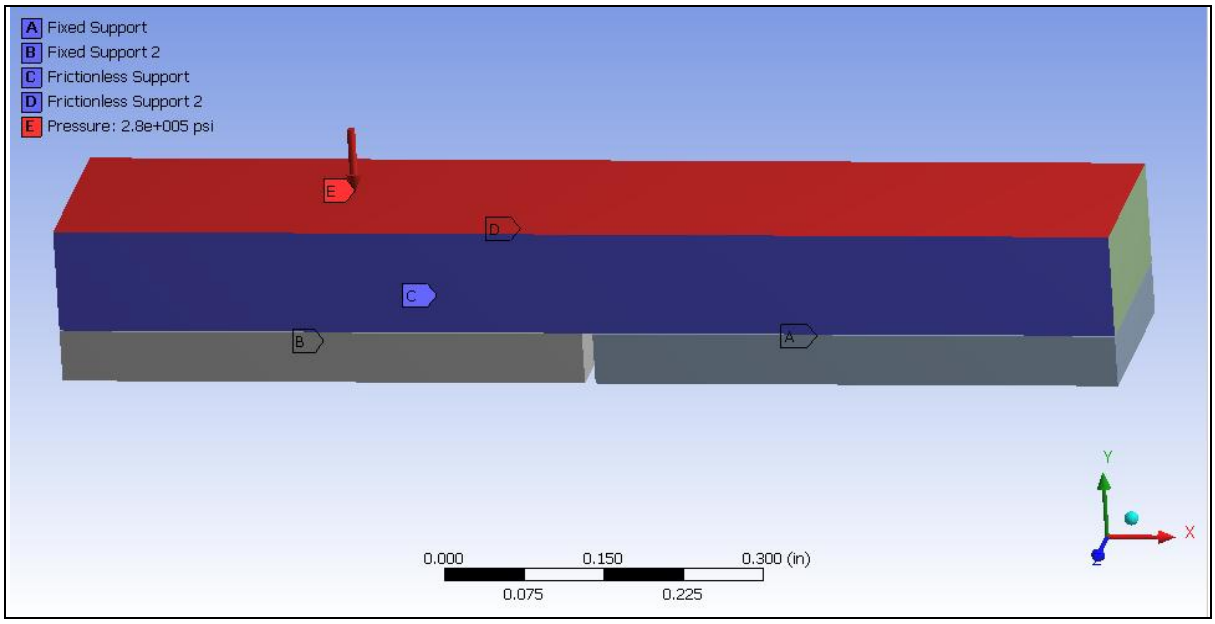

Figure 17. ANSYS model for deformation study.

The constant-z surfaces of the Stellite 25 block are provided a frictionless support, while the constant-x surfaces are allowed to deform freely. The ends of the block are far from the center of the block as compared to the gap width so that there will be little effect on the local deformation near the groove. The steel is treated as a perfectly elastic support, while the Stellite 25 is assumed to be elastic-perfectly plastic. Fixed supports on the bottom surfaces of the steel supports keep them from displacing. An element size of 0.0254 mm (0.001 in) was chosen for the Stellite 25 in the vicinity of the gap. Therefore, there were ten elements to capture the deformation of the Stellite 25 in this region.

The gap width of 0.254 mm (0.010 in) was chosen to represent a surface opening associated with a relatively wide and deep (~15–20 mil) groove in the steel. It is larger than the actual grooves and is meant to provide the possibility of a large deformation of the Stellite 25. Actual deformations would probably be smaller than those calculated, given a shallower and narrower groove in the steel cylinder.

A local coordinate system was established for the model near the bottom surface of the Stellite 25 block. It was centered in the middle of the gap and equidistant from the sides of the Stellite 25 block. It had the same orientation as the global coordinate system. The results of the calculations gave the magnitude of the deformation of the Stellite 25 block along a path coincident with the x-axis of the local coordinate system.

Figure 18 gives the results of the calculations for three applied pressures. Only the data in the vicinity of the gap are shown. The vertical lines shown in the plot are the bounds of the gap.

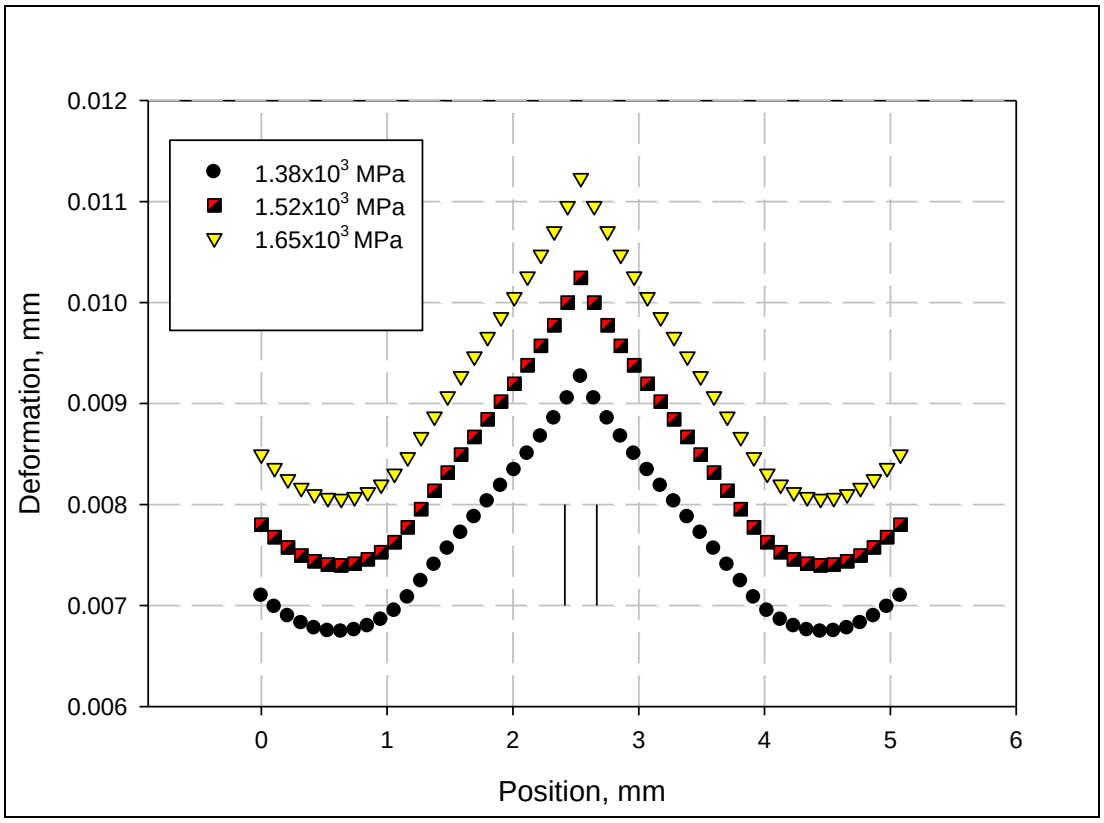

Figure 18. Calculated total deformation of Stellite 25 into gap.

The deformation also includes the elastic portion due to the applied pressure. Thus, the actual plastic deformation into the gap is less than the maximum deformation shown in the figure.

4.3 Plasticity Considerations

The ANSYS modeling of the steel cylinder shows that while the applied pressure is constant along a portion of the internal surface of the cylinder, the resulting stress state inside the cylinder varies considerably. This produces the variation in the measured and calculated hoop strain on the exterior of the cylinder. If the cylinder could be pressurized along its entire interior surface, the internal stress state would be somewhat simpler, since the only major complications would be from end effects. Given a very long cylinder, the end effects could be minimized.

Fundamental considerations of plasticity can be used to calculate the internal pressure P necessary to yield the entire volume of the cylinder (*8*). The assumption is that the cylinder is long and that there are no end effects. Also, the approximation is that the steel is elastic-perfectly plastic. In this case,

$$P = Y \ln(b/a), \tag{2}$$

where Y is the yield strength of the steel, a is the inner radius of the cylinder, and b is the outer radius. For an inner radius of 10.287 mm (0.405 in), an outer radius of 38.1 mm (1.5 in), and a yield strength of 1.16×10^3 MPa, we get $P = 1.52\times10^3$ MPa. Given the usual hydrostatic assumption, a load of 5.07×10^5 N would yield the entire cylinder.

The last three cylinders tested (5, 6, and 7) had loads in excess of this amount. However, these cylinders were arguably too short to produce a constant strain along a significant length of cylinder. However, this value of P may represent a lower bound for that needed to yield the entire cylinder.

5. Discussion

The major thrust of this effort has been to try to increase the strength of the bond between the liner and gun tube that is produced by the GLEEM process. It is therefore reasonable to ask what bond strength is actually necessary. Long and expensive firing tests of actual hardware is required to answer this question with certainty. However, some estimates can be made if some simple assumptions are made. One such estimate has been made in the case of the liner in the M2 machine gun (a 2007 report by de Rosset, et al.) (*9*). In this report the assumption was that the bond strength had to be large enough to overcome the reaction force from the torque that the liner applied to the bullet to spin it up. A bond strength of 4.8×10^4 Pa (7 psi) was estimated to be able to resist the reaction forces.

More recently, the force it takes to push a projectile down a barrel has been measured (*10*). It was found that a force of (at most) 2.5 kN was required to push a 5.56-mm bullet down the gun tube at a rate of 99 mm/s. Faster rates required a lower force. The bond between the liner and gun tube would have to resist this force. Assume that the liner is ½-mm thick. The liner's outer diameter would then be 6.56 mm. The outer surface area of the liner would be 10470 mm^2, assuming a 20-in (508-mm) barrel length. (Here, we assume the entire length of the barrel is lined. A shorter liner would need a stronger bond.) Thus, the shear stress to be overcome is $2500N/10470mm^2 = 2.38\times10^5$ Pa, or 35 psi.

Some reasonable assumptions can be made to scale up the force needed to be overcome for a 25-mm barrel. First, we assume that the pressure required to push the bullet down the tube remains the same. Second, we assume the liner for the larger tube has a proportionally greater thickness. That is, the medium caliber tube liner has a thickness of (25.4/5.56) × 0.5 mm = 2.27 mm. The pressure on the base of the small-caliber bullet is simply the applied force divided by the cross-sectional area of the bullet. This gives a pressure of 1.03×10^2 MPa. The same pressure applied to the base of the medium caliber bullet results in a force of 5.22×10^4 N. The resulting shear stress on the liner is calculated to be 3.03×10^5 Pa (44 psi), assuming a 1830-mm (6-ft) barrel length. This would be the estimated required minimum bond strength for

the medium caliber gun liner. This bond strength is two orders of magnitude less than that achieved with the advanced GLEEM process and makes this process appear to have potential for success.

The bond produced by the GLEEM process is frictional in nature. Its shear strength is a product of the force normal to the surface and the static coefficient of friction. The force normal to the bond interface is directly related to the residual stress produced by the plastic deformation caused by the applied pressure. The major contributor to the static coefficient of friction is the surface roughness. The data can be discussed in terms of both these factors.

The first conclusion drawn from this work is that for this particular combination of materials, the groove depth did not affect the strength of the bond. This is shown graphically in figure 19 for cylinders 1–4. With the exception of cylinder 2, all of these cylinders had the same maximum applied load and a bond strength in the range of 18 to 23 MPa. The larger bond strength for cylinder 2 might be attributed to the excursion in the load to 4.95×10^5 N. Note, however, that all four cylinders had maximum hoop strains at their centers that were about equal, so the load excursion cannot be the entire explanation.

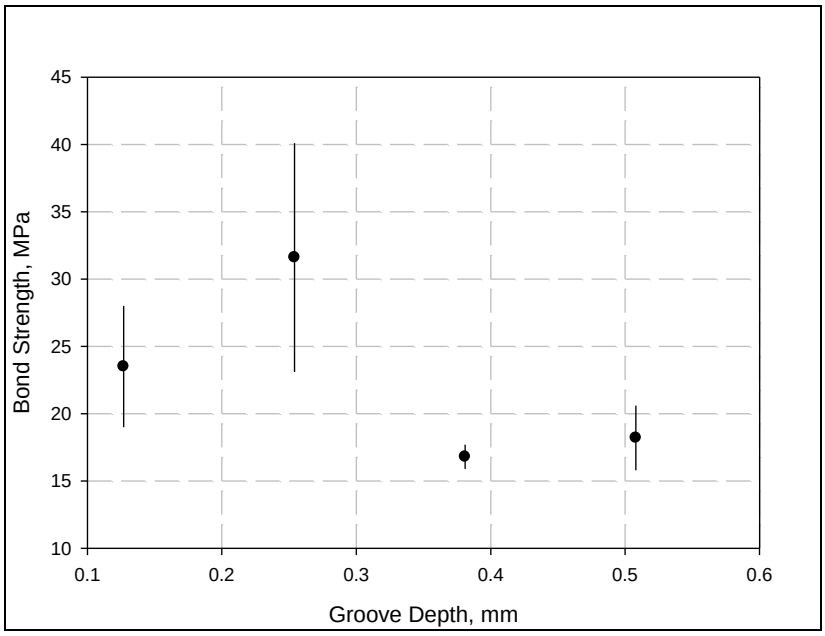

Figure 19. Graphical comparison of bond strengths for cylinders 1–4.

Examining the Stellite 25 liners after the GLEEM process had been applied to the cylinders showed that with the exception of the area of the liner near the piston face, there was no embossment of the Stellite 25 due to the machined grooves in the steel. It was assumed that the pressure had not been high enough to deform the Stellite, so the last three cylinders were tested with the intention of going to higher pressures. The 0.254-mm groove depth was chosen for all three cylinders based on the apparent success of this depth in creating a good bond (cylinder 2). In addition, the twist rate was increased to allow a greater surface area of groove to be present.

These experiments showed that even at higher pressures, there was very little movement of the Stellite 25 into the grooves. This finding was supported by ANSYS calculations that indicated the Stellite 25 would not fill a 0.254-mm wide groove even at the highest pressures applied during the experiments. Figures 6 and 8 show that the Stellite 25 conformed to the machined surface of the steel cylinder. However, the amount of Stellite deformation in these cases is small.

The second set of experiments (last three cylinders) produced higher bond strengths than the first set, with the exception of cylinder 2 as previously noted. As shown in the 2010 report by de Rosset (*2*), the residual stress, a factor in the bond strength, is proportional to the applied pressure. The plastic strain is also a function of the applied pressure. The second set of cylinders had larger final outer and inner diameters than those from the first set, which is consistent with the higher bond strengths in the second set of cylinders (see figures 5, 7, and 9.) The differences in material strength between the first and second set of cylinders also contributed to the larger plastic deformation in the second set of cylinders (see table 2).

The second set of experiments led to the conclusion that Teflon is a superior material to use as the elastomer in the GLEEM process. Figure 15 compares the hoop strains for the cylinders with Silastic or Teflon as the elastomer. The hoop strains for both cylinders go through a maximum, but the breadth of the maximum appears to be larger for the Teflon. The sharper drop-off in the hoop strain for the cylinder with Silastic may be due to greater frictional effects. However, a comparison of the experimental curves in this figure with the calculated results indicates that friction may be reducing the applied pressure for both materials for axial positions >100 mm. That is, the calculated values of the hoop strain begin to rise for axial positions >110 mm, but the measured values of hoop strains for both the Silastic- and Teflon-loaded cylinders decrease in this region.

Increasing the applied load indefinitely does not lead to higher residual stresses and increasingly higher bond strengths. (There is also the limitation on the inexpensive but effective seals used in the GLEEM process.) Eventually, the entire cylinder will yield, and a limit to the residual stress will be reached. This may have occurred with the current series of experiments. A hoop strain on the outer surface of 0.3% implies even higher hoop strains in the interior of the steel cylinder. The measurements of the inner diameters of the liners show radial strains more than 2% (figures 5 and 7). Thus, the interior radial and hoop strains are beyond the 0.2% offset generally used to mark the onset of plastic deformation.

The different elastomers used for this series and the different material strengths of the steel cylinders make a comparison the test results problematic. These differences may be of second order significance when compared to the effect that the maximum applied pressure has on the

measured bond strength as shown in figure 20. In this figure, the maximum pressure is that calculated from equation 1 using the maximum load. If the high data point at 1873 MPa is ignored, the plot suggests that there is a maximum in the bond strength somewhere between 1500 and 1700 MPa. In any event, pressures above 1500 MPa do not appear to provide any significant increase in bond strength.

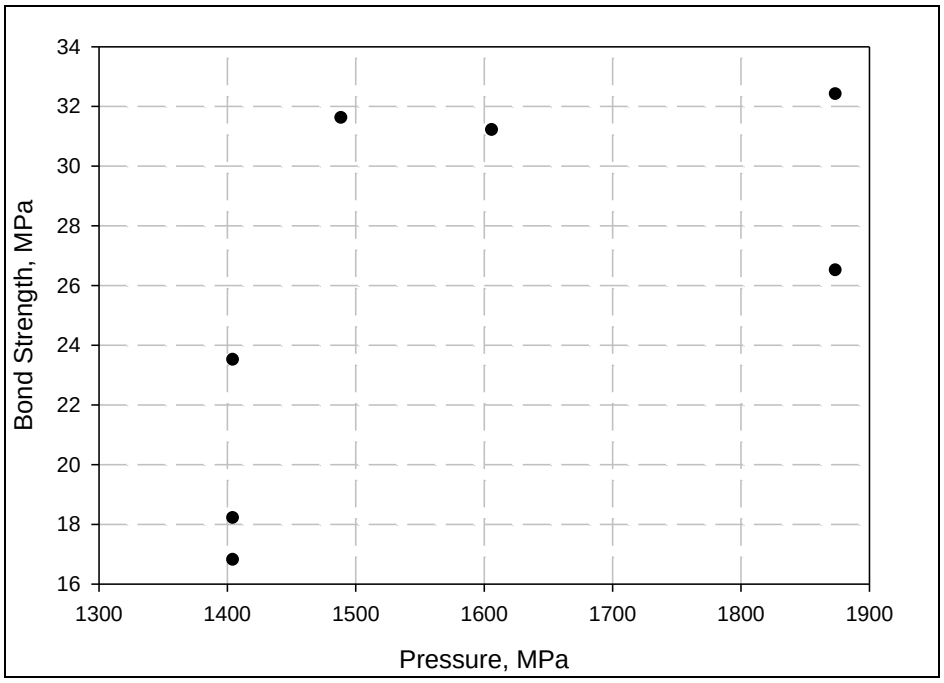

Figure 20. Comparison of bond strengths as a function of maximum applied pressure.

6. Summary

The major conclusions that can be drawn from this work are the following:

1. The applied load was not large enough to cause any significant penetration of the Stellite 25 liner into the grooves cut into the steel cylinder.
2. Teflon is the elastomeric material of choice for the GLEEM process.
3. For this particular combination of materials and geometry, bond strengths on the order of 30 MPa can be achieved by applying a pressure between 1500 and 1700 MPa.
4. Simple calculations indicate that bond strengths on the order of 0.3 MPa would be sufficient to resist the frictional forces produced by a bullet being pushed down a 25-mm gun tube.

7. References

1. Carter, R. H.; de Rosset, W. S.; Gray, D. M. GLEEM – A New Composite Gun Tube Processing Technology. In *Proceedings of the 26th Annual Army Science Conference*, Orlando, FL, December 2008.

2. de Rosset, W. S. *Gun Liner Emplacement with an Elastomeric Material*; ARL CR-645; U.S. Army Research Laboratory: Aberdeen Proving Ground, MD, April 2010.

3. Carter, R. H.; de Rosset, W. S. Compressed Elastomer Method for Autofrettage and Lining Tubes. U.S. Army Research Laboratory Patent Application 12/176,608, July 2008.

4. de Rosset, W. S.; Snoha, D. J.; Minnicino, M. A. *Strength of an Explosively-Formed Bond*; ARL-TR-3889; U.S. Army Research Laboratory: Aberdeen Proving Ground, MD, September 2006.

5. Gray, D. *GLEEM Testing Fixture*; ARL-TN-360; U.S. Army Research Laboratory: Aberdeen Proving Ground, MD, July 2009.

6. Chu, T. C.; Ranson, W. F.; Sutton, M. A.; Peters, W. H. Applications of Digital-Image-Correlation Techniques to Experimental Mechanics. *Experimental Mechanics* **September 1985**, 232–244.

7. www.carbidedepot.com/formulas-hardness (accessed March 9, 2010).

8. Calladine, C. R. *Engineering Plasticity*; Pergamon Press, Ltd.: London, England, 1969, 76.

9. de Rosset, W. S.; Montgomery, J. S. *Machine Gun Liner Bond Strength*; ARL-CR-595; U.S. Army Research Laboratory: Aberdeen Proving Ground, MD, August 2007.

10. South, J.; Yiournas, A.; Wagner, J.; Brown, J.; Kaste, R. *A Study of the Engraving of the M855 5.56-mm Projectile*; ARL TR-4743; U.S. Army Research Laboratory: Aberdeen Proving Ground, MD, March 2009.

Appendix. Experimental Details

Table A-1. Detailed measurements on sectioned samples.

Cylinder No.	Slice No.	Liner Outer Diameter (mm)	Liner Thickness (mm)	Maximum Load (N)	Bond Shear Strength (Pa)
1	1	25.55	5.055	11751	28.96
	2	25.48	5.055	6961	17.21
	3	25.58	5.055	8722	21.47
	4	25.53	5.055	10680	26.34
2	1	25.45	5.055	13638	33.74
	2	25.53	5.029	17592	43.61
	3	25.53	5.055	11823	29.16
	4	25.55	5.105	8153	19.89
3	1	25.50	5.055	7308	18.05
	2	25.45	4.953	6583	16.59
	3	25.45	5.055	6298	15.58
	4	25.48	5.055	6863	16.96
4	1	25.48	5.029	6494	16.13
	2	25.48	5.055	8994	22.23
	3	25.45	5.055	6708	16.60
	4	25.43	5.054	7143	17.69
5	1	25.68	4.877	10573	26.87
	2	25.65	4.928	13042	32.84
	3	25.68	4.877	11916	30.29
	4	25.55	4.902	13731	34.89
6	1	25.83	5.08	13264	32.17
	2	25.83	5.08	13028	31.60
	4	25.68	5.08	13687	33.39
7	1	25.86	5.08	9434	22.86
	2	25.81	5.08	11338	27.53
	4	25.81	5.105	12081	29.19

NO. OF
COPIES ORGANIZATION

1 (PDF only) DEFENSE TECHNICAL INFORMATION CTR
DTIC OCA
8725 JOHN J KINGMAN RD
STE 0944
FORT BELVOIR VA 22060-6218

1 DIRECTOR
US ARMY RESEARCH LAB
IMNE ALC HRR
2800 POWDER MILL RD
ADELPHI MD 20783-1197

1 DIRECTOR
US ARMY RESEARCH LAB
RDRL CIM L
2800 POWDER MILL RD
ADELPHI MD 20783-1197

1 DIRECTOR
US ARMY RESEARCH LAB
RDRL CIM P
2800 POWDER MILL RD
ADELPHI MD 20783-1197

1 DIRECTOR
US ARMY RESEARCH LAB
RDRL D
2800 POWDER MILL RD
ADELPHI MD 20783-1197

1 DIRECTOR
US ARMY RESEARCH LAB
RDRL WML G A ABRAHAMIAN
2800 POWDER MILL RD
ADELPHI MD 20783-1197

1 DIRECTOR
US ARMY RESEARCH LAB
RDRL WML G M BERMAN
2800 POWDER MILL ROAD
ADELPHI MD 20783-1197

ABERDEEN PROVING GROUND

1 DIR USARL
RDRL CIM G (BLDG 4600)

NO. OF COPIES ORGANIZATION

1 OFC DEPUTY UNDER SEC DEF
J THOMPSON
1745 JEFFERSON DAVIS HWY
CRYSTAL SQ 4 STE 501
ARLINGTON VA 22202

1 COMMANDER
US ARMY MATL CMND
AMXMI INT
9301 CHAPEK RD
FT BELVOIR VA 22060-5527

1 PM ARMS
SFAE AMO MAS MC
BLDG 354
PICATINNY ARSENAL NJ
07806-5000

1 COMMANDER
US ARMY ARDEC
AMSRD AAR AEM D
J LUTZ
BLDG 354
PICATINNY ARSENAL NJ
07806-5000

1 COMMANDER
US ARMY ARDEC
AMSRD AAR ATD
B MACHAK
BLDG B1
PICATINNY ARSENAL NJ
07806-5000

1 PM MAS
SFAE AMO MAS
CHIEF ENGR
PICATINNY ARSENAL NJ
07806-5000

1 COMMANDER
US ARMY TACOM
PM COMBAT SYS
SFAE GCS CS
6501 ELEVEN MILE RD
WARREN MI 48397-5000

1 US ARMY RDECOM-TARDEC
SURVIVABILITY HEAD MRAP
JPO PEO-GROUND COMBAT SYS
AMSTA TR R
D TEMPLETON
6501 ELEVEN MILE RD
WARREN MI 48397-5000

NO. OF COPIES ORGANIZATION

1 PM STRYKER
SFAE GCS BCT
M RYZYI
6501 ELEVEN MILE RD
WARREN MI 48397-5000

1 PM-HEAVY BRIGADE
COMBAT TEAM
SFAE CGSS W AB QT
J MORAN
6501 ELEVEN MILE RD
WARREN MI 48397-5000

1 DARPA
S WAX
3701 N FAIRFAX DR
ARLINGTON VA 22203-1714

1 DIRECTOR
NGIC
IANG TMT
2055 BOULDERS RD
CHARLOTTESVILLE VA 22911

3 DIRECTOR
BENET WEAPON LABS
RDAR WSB
M AUDINO
M MILLER
F CAMPO
WATERVLIET ARSENAL
WATERVLIET NY 12189-4000

39 DIR USARL
RDRL LOA F
M ADAMSON
RDRL WM
B FORCH
J MCCAULEY
P PLOSTINS
J SMITH
RDRL WML
M ZOLTOSKI
J NEWILL
RDRL WML A
T KOGLER
RDRL WML B
R LIEB
R PESCE-RODRIGUEZ
B RICE
RDRL WML D
P CONROY

NO. OF
COPIES ORGANIZATION

RDRL WML G
W DRYSDALE
M MINNICINO
RDRL WMM
R DOWDING
H MAUPIN
RDRL WMM A
R EMERSON
RDRL WMM B
T BOGETTI
B CHEESEMAN
D GRAY
RDRL WMM D
E CHIN
D GRANVILLE
W ROY
RDRL WMM E
J LASALVIA
J SWAB
RDRL WMM F
R CARTER
W DE ROSSET
L KECSKES
J MONTGOMERY
D SNOHA
RDRL WMP
P BAKER
S SCHOENFELD
RDRL WMP B
C HOPPEL
RDRL WMP C
T BJERKE
RDRL WMP D
T HAVEL
J RUNYEON
RDRL WMP E
M BURKINS

INTENTIONALLY LEFT BLANK.